Journal of Nuclear Medicine, published on June 21, 2024 as doi:10.2967/jnumed.124.267774

Dose–Response Relationship in Patients with Liver Metastases from Neuroendocrine Neoplasms Undergoing Radioembolization with ^{90}Y Glass Microspheres

Masao Watanabe[1,2], Stephan Leyser[1,2], Jens Theysohn[2,3], Benedikt Schaarschmidt[2,3], Johannes Ludwig[4], Wolfgang P. Fendler[1,2], Alexandros Moraitis[1,2], Harald Lahner[5], Annie Mathew[5], Ken Herrmann[1,2], and Manuel Weber[1,2]

[1]Department of Nuclear Medicine, University Clinic Essen, Essen, Germany; [2]University of Duisburg–Essen and German Cancer Consortium–University Hospital, Essen, Germany; [3]Institute of Diagnostic and Interventional Radiology and Neuroradiology, University Clinic Essen, Essen, Germany; [4]Department of Radiology and Nuclear Medicine, University Medical Center Mannheim, Heidelberg University, Mannheim, Germany; and [5]Department of Endocrinology, Diabetes, and Metabolism and Division of Laboratory Research, University Clinic Essen, Essen, Germany

The benefit of multicompartment dosimetry in the radioembolization of neuroendocrine neoplasms is not firmly established. We retrospectively assessed its potential with patient outcome. **Methods:** Forty-three patients were eligible. The association of mean absorbed dose (MAD) for tumors and treatment response was tested per lesion with a receiver operating characteristic curve analysis, and the association of MAD with progression-free survival (PFS) and overall survival was tested per patient using uni- and multivariate Cox regression analyses. **Results:** The area under the curve for treatment response based on MAD was 0.79 (cutoff, 196.6 Gy; $P < 0.0001$). For global PFS, grade (grade 2 vs. 1: hazard ratio [HR], 2.51; $P = 0.042$; grade 3 vs. 1: HR, 62.44; $P < 0.001$), tumor origin (HR, 6.58; $P < 0.001$), and MAD (HR, 0.998; $P = 0.003$) were significant. For overall survival, no prognostic parameters were significant. **Conclusion:** In line with prior publications, a MAD of more than 200 Gy seemed to favor treatment response. MAD was also associated with PFS and may be of interest for radioembolization planning for neuroendocrine neoplasm patients.

Key Words: radioembolization; neuroendocrine neoplasm; multicompartment dosimetry

J Nucl Med 2024; 00:1–6
DOI: 10.2967/jnumed.124.267774

Neuroendocrine neoplasms (NENs) are metastatic at initial diagnosis in up to 85% of patients with pancreatic NENs and 90% of those with small-intestine NENs, with the liver being the organ mainly affected (*1*), which negatively impacts survival and potentially leads to hormonal excess due to a lack of hepatic first-pass effect (*2*).

Radioembolization is an effective and safe treatment for primary liver tumors (e.g., hepatocellular carcinoma) and for liver metastases secondary to, for example, colorectal carcinoma or NENs (*2–5*). For the latter, radioembolization is mentioned as a treatment option, especially in the context of large lesions, hormonally active tumors, and somatostatin-receptor–negative tumors (*1,2,6*).

In many previous trials on radioembolization in NENs, activity was routinely calculated by use of single-compartment dosimetry, that is, based on average values to the perfused target tissue (*2*). However, in recent years, a benefit with regard to progression-free survival (PFS) and overall survival (OS) could be shown in hepatocellular carcinoma patients when using multicompartment modeling, that is, optimizing doses to the tumor and nontumor tissue by separately assessing average doses to these 2 compartments (*7*). Therefore, this approach is also recommended in the new European Association of Nuclear Medicine guidelines on treating liver tumors (*5*). The doses to each compartment are derived from pretherapeutic ^{99m}Tc-macroaggregated albumin (MAA) SPECT (*5*), which has been shown to be an imperfect but moderately reliable surrogate for ^{90}Y microsphere dose distribution.

For NENs, evidence on the association of multicompartment dosimetry and patient outcome is scarce (*8,9*). In addition, safety doses for nontumor liver tissue have not been established.

We therefore aimed to assess the association of dosimetry parameters derived from multicompartment dosimetry on the one hand and patient outcome on the other hand in patients with NENs by performing a retrospective analysis of patients treated in our institution.

MATERIALS AND METHODS

Patients

From June 2007 to April 2022, 99 consecutive patients were retrieved from our radioembolization database, of whom 43 could be enrolled for this retrospective study. The patient enrollment process is summarized in Figure 1, and the patient characteristics are summarized in Table 1.

To be included, patients had to have undergone radioembolization for the treatment of hepatic metastases secondary to NENs with no other organs being affected, or with extrahepatic spread being judged as prognostically irrelevant, or with hormone-associated symptoms being insufficiently controlled pharmacologically. The exclusion criteria were incomplete treatment records on radioembolization including ^{99m}Tc-MAA SPECT/CT and contrast-enhanced CT or enhanced MRI, untreated liver lesions after radioembolization, and unavailable information on the Ki-67 index of the tumor or PFS.

All analyses were performed in accordance with the principles laid out in the Declaration of Helsinki and its later amendments and approved by the institutional review board of the Medical Faculty of the University

Received Mar. 13, 2024; revision accepted May 30, 2024.
For correspondence or reprints, contact Masao Watanabe (d7he4ng@gmail.com).
Published online Jun. 21, 2024.

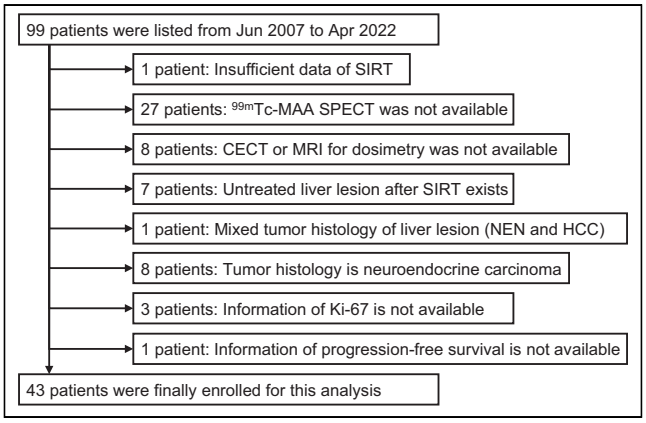

FIGURE 1. Consort diagram of patient enrollment. CECT = contrast-enhanced CT; HCC = hepatocellular carcinoma; SIRT = selective internal radiation therapy.

Duisburg–Essen (approval 13-5325BO). All patients gave written informed consent for the analysis of available data.

Image Acquisition and Treatment Algorithm

A median of 150.0 MBq (range, 147.0–163.0 MBq) of ^{99m}Tc-MAA was administered into the hepatic target vessels, and image acquisition started within 2 h. Details regarding the acquisition protocol, image reconstruction, and interpretation have been published previously (*10*). Treatment activity was calculated using unicompartment dosimetry, mostly aiming at a mean absorbed dose (MAD) to the perfused target volume of between 80 and 150 Gy (*5*).

Dosimetry Procedure

Post hoc multicompartment dosimetry was performed by a board-certified nuclear medicine physician and radiologist using Simplicit90Y (Mirada Medical).

After manual coregistration of contrast-enhanced CT or MRI and ^{99m}Tc-MAA SPECT/CT images, segmentation of whole-liver volume, perfused target volumes, tumor tissue, and nontumor liver tissue was performed both manually and automatically or semiautomatically by use of the tools "Liver Segmentation" and "Region with % of Max." Segmentation of the whole liver volume was performed automatically, whereas tumor lesions were segmented on ^{99m}Tc-MAA SPECT using visually determined thresholds, since optimal coregistration with the diagnostic CT or MRI was severely impeded in many patients because of multifocal disease.

Most but not all tumors displayed a high tumor–to–normal-tissue ratio; in these cases, a percentage-based threshold was placed around the tumor to delineate the hypervascular part. In line with a round-robin study (*11*), this threshold was chosen individually for each patient, since fixed thresholds may induce systematic errors in the volumetric assessment of lesions with different uptake levels. In the remainder, that is, tumors with very low tumor–to–normal-tissue ratios, the delineation was performed manually.

On the basis of prior publications, we measured the MAD for tumor on a per-lesion and per-patient basis (*9*).

To evaluate prognostic factors for liver toxicity after radioembolization, we calculated the MAD to the whole nontumor liver tissue using multicompartment dosimetry (*10*).

Evaluation of Tumor Response to Selective Internal Radiation Therapy

We evaluated baseline and the first follow-up contrast-enhanced CT images using the criteria of Choi et al. (*12*), in consideration of prior publications demonstrating its suitability for response assessment in NEN patients (*13*). Up to 10 lesions per patient were selected, and the anatomic location of each tumor across contrast-enhanced CT and ^{99m}Tc-MAA SPECT/CT was precisely recorded, with a preference for bigger and well-marginated lesions to avoid individual patient bias. To avoid the partial-volume effect, lesions smaller than 2 cm were excluded from lesion-based analyses (*14*). Eight patients did not have lesions 2 cm or larger, and the follow-up enhanced CT was not available in 7 patients. Finally, 28 patients were eligible for this response evaluation. Lesions were classified into the categories of complete remission (CR), partial response (PR), stable disease (SD), and progressive disease (PD). We also categorized the lesions as responding (CR + PR) or nonresponding (SD + PD) (*12*). In the 28 patients eligible for lesion-based response analysis, the median interval between the baseline imaging and radioembolization, between radioembolization and the first follow-up imaging, and between baseline imaging and the first follow-up imaging was 2 mo (range, 1–5 mo), 4 mo (range, 1–6 mo), and 6 mo (range, 2–9 mo), respectively.

Follow-up

All patients were followed up for OS and PFS (using RECIST 1.1) until August 2023. All patients underwent cross-sectional imaging as part of the follow-up imaging. The imaging interval was based on the treating physician's decision, typically every 3 mo, rarely (e.g., in slowly growing tumors) less frequently.

In addition, 29 patients could be followed up using aspartate aminotransferase, alanine aminotransferase, total bilirubin measurements, and albumin for at least 12 mo. Adverse events were graded using the Common Terminology Criteria for Adverse Events (CTCAE) version 5. Relevant liver toxicity was defined as a binary metric by the occurrence of grade 3+ toxicity in aspartate aminotransferase, alanine aminotransferase, bilirubin, and albumin levels, based on prior publications identifying it as a particularly suitable marker for liver toxicity after radioembolization (*9*).

Statistical Analysis

We used the Mann–Whitney *U* test to compare MAD among lesions with CR, PR, SD, and PD. To determine the model fit and a cutoff between responding and nonresponding lesions, we performed a receiver operating characteristic curve analysis with the Youden index, as well as the hepatic response per patient. We calculated the sensitivity, specificity, positive predictive value, negative predictive value, and accuracy for the lesion-based response and the patient-based hepatic response.

A proportional-hazards regression analysis (Cox analysis) was performed for hepatic PFS, global PFS, and OS using MAD per patient; grade 1 (G1), grade 2 (G2), and grade 3 (G3); and tumor origin (pancreatic vs. other origins). Prognostic factors with *P* values of less than 0.05 in the univariate analysis entered the multivariate analysis.

To investigate the difference in hepatic response and MAD per patient with regard to NEN grading, we performed the χ^2 (Cochran–Armitage) test for trend and the Kruskal–Wallis test, respectively.

For these analyses, we used Prism version 8 (GraphPad Software) and MedCalc version 22.014 (MedCalc Software). A *P* value of less than 0.05 was regarded as statistically significant.

RESULTS

Patients

Of 99 initially available patients, 36 were excluded because of insufficient data (e.g., ^{99m}Tc-MAA SPECT/CT or contrast-enhanced CT or MRI) for dosimetry. Seven patients had untreated liver lesions after radioembolization, and 9 patients were excluded because of the tumor histology (NEN and hepatocellular carcinoma, $n = 1$; neuroendocrine carcinoma, $n = 8$). Four patients did not have enough clinical data for the survival analysis. Finally, 43 patients were eligible for our study.

TABLE 1
Patient Characteristics (n = 43)

Clinical variable	Value
Age (y)	Median, 60; range, 35–77
Male/female (*n*)	24/19
Origin of tumor: pancreas/gastrointestinal/unknown	11/30/2
NEN grade: 1/2/3	14/26/3
Endocrine syndrome: positive/negative (*n*)	12/31
Liver cirrhosis: positive/negative (*n*)	1/42
Extrahepatic lesions: positive/negative (*n*)	19/24
Number of involved regions: 1/2/3/4 (*n*)*	12/4/2/1
Lymph node/thyroid gland/lung (*n*)	14/1/3
Adrenal gland/peritoneum/ovary/bone (*n*)	1/5/2/4
Partial-liver/whole-liver SIRT (*n*)	6†/37
Sessions for whole-liver SIRT: 1/2 (*n*)	29/8
Treated volume (mL)	Median, 1,735.4; range, 828.6–6,377.3
Treated fraction (%)	Median, 100; range, 61.4–100
Administered dose (GBq)	Median, 3.9; range, 2.1–22.0
MIRD dose (Gy)	Median, 107.1; range, 44.8–164.3
MAD (Gy)	Median, 219.5; range, 48.1–1014.6
Perfused volume normal-tissue AD (Gy)	Median, 96.2; range, 13.7–181.0
Whole-liver normal-tissue AD (Gy)	Median, 95.3; range, 13.6–181.1
Lung shunt fraction (%)	Median, 2.9; range, 0.7–29.0
PV thrombosis: Vp1–Vp3/Vp4/negative (*n*)	1/0/42
Prior therapy (*n*)	40
Number of therapies: 0/1/2/3/4/5 (*n*)‡	3/9/11/11/4/5
Tumor resection: primary/liver metastasis (*n*)	34/8
TACE/RFA/radiotherapy (*n*)	5/3/1
Somatostatin/PRRT/systemic therapy (*n*)	29/12/13
After SIRT (*n*)	38
Number of therapies: 0/1/2/3/4/5 (*n*)‡	5/17/14/4/2/1
Tumor resection: primary/liver metastasis (*n*)	1/2
TACE/RFA/radiotherapy (*n*)	2/0/0
Somatostatin/PRRT/systemic therapy (*n*)	28/16/18
Additional SIRT (≥6 mo later) (*n*)	3

*Number of involved regions per patient.
†Four and 2 patients underwent radioembolization for right lobe and right lobe plus medial segment, respectively.
‡Number of therapies per patient.
SIRT = selective internal radiation therapy; AD = absorbed dose; PV = portal vein; TACE = transarterial chemoembolization; RFA = radiofrequency ablation. PRRT = peptide receptor radionuclide therapy; systemic therapy = mammalian target of rapamycin inhibitor or chemotherapy.

Of 37 patients (37/43, 86.0%) who underwent whole-liver radioembolization, 29 (78.4%) underwent single-session radioembolization and 8 (21.6%) underwent sequential treatment 4–6 wk apart. In the remaining 6 patients who underwent single-session partial-liver radioembolization (right liver in 4 patients, right liver including segment 4 in the remainder), the median fraction of treated liver volume was 73.0% (range, 61.4%–93.0%). In 43 of a total of 51 treatment sessions, the microspheres were used within 7 d after calibration; in the remainder, after more than 7 d. The median duration between calibration and radioembolization was 4 d (range, 2–11 d).

Lesion-Based Tumor Response Analysis

Of 28 eligible patients for the response evaluation, 21 (75.0%) responded (CR + PR) in the follow-up imaging. The median hepatic PFS, global PFS, and OS of the eligible subcohort for the response analysis were 11 mo (range, 1–73 mo), 10.5 mo (range, 1–73 mo), and 28 mo (range, 2–115 mo), respectively.

In 28 eligible patients who had liver lesions 2 cm or larger, 126 lesions were available for lesion-based analyses. There were 85 responding and 41 nonresponding lesions; 14 of the latter progressed despite treatment.

Median values for responding versus nonresponding lesions were 237.6 Gy (range, 52.7–1178.0 Gy) and 120.2 Gy (range, 29.9–424.9 Gy) for MAD (area under the curve, 0.79; cutoff, 196.6 Gy; $P < 0.0001$). The sensitivity, specificity, positive predictive value, negative predictive value, and accuracy were 64.7% (55/85), 85.4% (35/41), 90.2% (55/61), 53.8% (35/65), and 71.4% (90/126), respectively.

Median values for patient-based hepatic response versus lack thereof were 268.7 Gy (range, 52.7–1,014.6 Gy) and 148.1 Gy (range, 78.8–284.6 Gy) for MAD (area under the curve, 0.78; cutoff, 175.0 Gy; $P = 0.003$). The sensitivity, specificity, positive predictive value, negative predictive value, and accuracy were 66.7% (14/21), 71.2% (5/7), 87.5% (14/16), 41.7% (5/12), and 67.9% (19/28), respectively.

The results including Mann–Whitney test and receiver operating characteristic analyses are summarized in Figures 2 and 3.

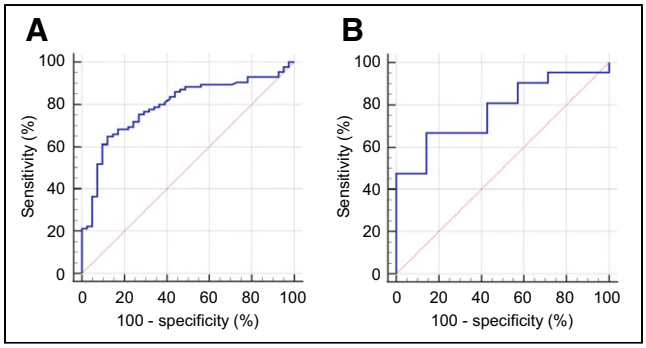

FIGURE 3. Receiver operating characteristic comparison of tumor response to radioembolization in terms of MAD for tumors to classify responder group vs. nonresponder group per lesion (A, 126 lesions) and per patient (B, 28 patients).

Survival Analysis

The median follow-up period was 34 mo (range, 2–151 mo). During this period, 35 of 43 (81.4%) patients died, 33 patients (76.7%) experienced global disease progression, and 24 patients (55.8%) experienced hepatic disease progression. The median hepatic PFS, global PFS, and OS of the entire cohort was 15 mo (range, 1–151 mo), 12 mo (range, 1–151 mo), and 34 mo (range, 2–151 mo), respectively.

The median MAD in all enrolled patients was 219.5 Gy (range, 48.1–1014.6 Gy).

In the univariate analysis for hepatic PFS, NEN grade (G2 vs. G1: hazard ratio [HR], 4.02; 95% CI of HR, 1.31–12.32; $P = 0.015$) and tumor origin (HR, 2.66; 95% CI of HR, 1.05–6.76; $P = 0.040$) were significant prognostic factors, whereas MAD was not. In the multivariate analysis, grade (G2 vs. G1: HR, 3.90; 95% CI of HR, 1.26–12.07; $P = 0.018$) and tumor origin (HR, 2.65; 95% CI of HR, 1.01–6.93; $P = 0.048$) were significant prognostic factors for shorter hepatic PFS. The results are shown in Table 2.

In the univariate analysis for global PFS, grade (G2 vs. G1: HR, 2.49; 95% CI of HR, 1.04–5.96; $P = 0.040$; G3 vs. G1: HR, 36.53; 95% CI of HR, 6.71–198.93; $P < 0.001$), tumor origin (HR, 2.47; 95% CI of HR, 1.14–5.33; $P = 0.021$), and MAD (HR, 0.998; 95% CI of HR, 0.997–1.000; $P = 0.0498$) were significant prognostic factors. In the multivariate analysis, grade (G2 vs. G1: HR, 2.51; 95% CI of HR, 1.04–6.09; $P = 0.042$; G3 vs. G1: HR, 62.44; 95% CI of HR, 9.96–391.48; $P < 0.001$), tumor origin (HR, 6.58; 95% CI of HR, 2.50–17.36; $P < 0.001$), and MAD (HR, 0.998; 95% CI of HR, 0.996–0.999; $P = 0.003$) were significant. These results are summarized in Table 2.

In the univariate Cox analysis for OS, grade (G3 vs. G1: HR, 3.88; 95% CI of HR, 1.03–14.63; $P = 0.045$) and MAD (HR, 0.998; 95% CI of HR, 0.996–1.000; $P = 0.049$) were significant prognostic factors. In the multivariate analysis for OS, no prognostic factors were significant. These results are summarized in Table 2.

Differences in hepatic response and MAD per patient with regard to NEN grading were not statistically significant ($P > 0.99$ and $P = 0.078$, respectively).

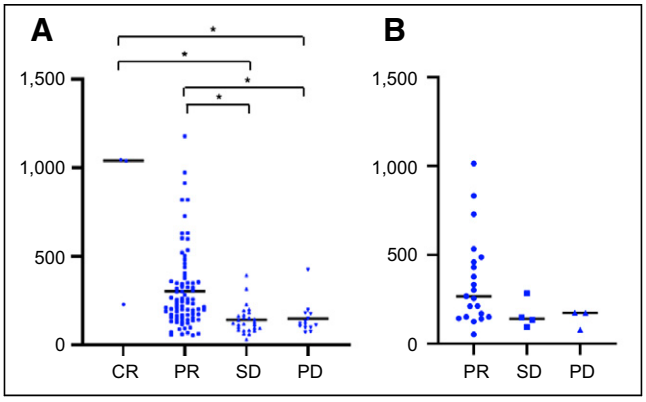

FIGURE 2. Lesion-based (A) and patient-based (B) comparisons of MAD for tumors among groups with CR, PR, SD, and PD. Horizontal line embedded in scatterplot is median value of each group. No CR response per patient was observed. There were no significant differences among PR, SD, and PD groups per patient. *$P < 0.01$; each value was compared using Mann–Whitney test.

Liver Toxicity After Radioembolization

Laboratory data were fully available for 29 patients for 12 mo after the radioembolization. During this interval, CTCAE grade 0, 1, 2, and 3+ liver toxicity was observed in 3, 23, 2, and 1 cases, respectively, based on elevated aspartate aminotransferase; in 10, 17, 1, and 1 cases, respectively, based on elevated alanine aminotransferase; in 17, 4, 7, and 1 cases, respectively, based on hyperbilirubinemia; and in 28, 0, 0, and 1 cases, respectively, based on hypoalbuminemia.

One patient experienced CTCAE grade 3+ hyperbilirubinemia and hypoalbuminemia within 6 mo after partial-liver radioembolization, and another patient experienced CTCAE grade 3+ elevated aspartate aminotransferase and alanine aminotransferase within 6 mo after whole-liver radioembolization. The nontumor liver tissue doses and the perfused normal-liver absorbed doses were 107.7 and 125.2 Gy in the former patient and 181.1 and 181.0 Gy in the other, respectively. Treatment after radioembolization consisted of somatostatin analogs in both patients, with 1 patient additionally receiving temozolomide 6–12 mo after radioembolization.

DISCUSSION

Our study showed a significant association between treatment response and absorbed doses in NEN patients treated with radioembolization. After excluding lesions smaller than 2 cm to reduce partial-volume effects, we could show that higher absorbed doses increased the likelihood of treatment response, with an MAD of 196.6 Gy per lesion and 175.0 Gy per patient being the most accurate predictor of treatment response. This threshold is in line with previously published target doses (*9*) and may serve for orientation in radioembolization planning in NENs; with the optimal cutoff

TABLE 2
Uni- and Multivariate Cox Proportional Hazards Regression Analyses for Hepatic and Global PFS and OS

		Univariate		Multivariate	
Survival type	Grade	HR	*P*	HR	*P*
Hepatic PFS	NEN grade				
	Grade 2 vs. 1	4.02 (1.31–12.32)	0.015	3.90 (1.26–12.07)	0.018
	Grade 3 vs. 1	3.74 (0.67–20.97)	0.13	4.43 (0.78–25.35)	0.094
	Tumor origin	2.66 (1.05–6.76)	0.040	2.65 (1.01–6.93)	0.048
	MAD	0.999 (0.997–1.001)	0.29		
Global PFS	NEN grade				
	Grade 2 vs. 1	2.49 (1.04–5.96)	0.040	2.51 (1.04–6.09)	0.042
	Grade 3 vs. 1	36.53 (6.71–198.93)	<0.001	62.44 (9.96–391.48)	<0.001
	Tumor origin	2.47 (1.14–5.33)	0.021	6.58 (2.50–17.36)	<0.001
	MAD	0.998 (0.997–1.000)	0.0498	0.998 (0.996–0.999)	0.003
OS	NEN grade				
	Grade 2 vs. 1	1.82 (0.85–3.86)	0.12	1.81 (0.84–3.87)	0.13
	Grade 3 vs. 1	3.88 (1.03–14.63)	0.045	3.15 (0.82–12.12)	0.095
	Tumor origin	1.93 (0.88–4.22)	0.099		
	MAD	0.998 (0.996–1.000)	0.049	0.998 (0.997–1.0002)	0.072

Data are for 43 patients and for 24, 33, and 35 events for hepatic PFS, global PFS, and OS, respectively. Data in parentheses are 95% CIs. Prognostic parameters with $P < 0.05$ in univariate analysis entered multivariate analysis.

for MAD (196.6 Gy) in our study, a response was noted in 55 of 61 (90.2%) lesions and 14 of 16 (87.5%) patients.

Higher tumor doses on a per-patient basis were also associated with longer global PFS despite not being a significant prognostic factor for hepatic PFS and OS. A possible explanation for this discrepancy lies in the considerable heterogeneity in our cohort, which included well-, intermediate-, and poorly differentiated NENs. As the degree of differentiation has been shown to be a significant predictor of both hepatic and global PFS in our cohort, this likely constitutes a confounding variable alongside other factors not accounted for in the multivariate analysis. In addition, patients may experience a significant overall reduction in hepatic tumor burden after radioembolization while still meeting the criteria for hepatic disease progression, for example, due to the occurrence of new lesions, thus potentially influencing results.

To our knowledge, so far only 2 other publications have assessed the association between tumor-absorbed dose and patient outcome in NEN patients (*8,9*) using multicompartment dosimetry. Ebbers et al. investigated the dose–response relationship after radioembolization with ^{90}Y glass microspheres using multicompartment dosimetry (*9*). For prediction of treatment response, they determined an optimal cutoff of 135 Gy for MAD, whereas 200 Gy predicted response with a higher specificity (*9*). Importantly, Ebbers et al. used ^{90}Y PET/CT for multicompartment dosimetry, which allows for an optimized assessment of the dose–response relationship, as it takes into account the doses administered during radioembolization, whereas pretherapeutic dose calculations by use of ^{99m}Tc-MAA have been shown to be inaccurate in a considerable fraction of patients (*9*). On the other hand, at least in the context of ^{90}Y microspheres, ^{99m}Tc-MAA is the only modality that enables pretherapeutic assessment of absorbed doses, thereby influencing dosing strategies more profoundly. In addition, because of the hypervascular nature of most NEN tumors, it seems likely that ^{99m}Tc-MAA can accurately predict posttreatment dose distribution, making the pretherapeutic dosimetry fairly reliable (*8*).

In our cohort, only 2 patients experienced CTCAE grade 3+ liver toxicity within 6 mo after radioembolization, with relatively high doses to the nontumor liver tissue and the perfused normal liver. As neither patient underwent hepatotoxic treatment within 6 mo after radioembolization, the hepatotoxicity was possibly caused by high absorbed doses to healthy liver tissue. Ebbers et al. reported grade 3+ liver toxicity in 3 of 30 patients in their cohort (*9*). A significant relationship between the absorbed dose in nontumor liver tissue and any biochemical toxicity of grade 3+ in logistic regression analysis could not be established (*9*). In addition, there are growing concerns among practitioners that radioembolization can lead to durable chronic hepatotoxicity and sometimes can be severely toxic (*15*). Currie et al. demonstrated that 4 of 28 patients (14%) experienced solely radioembolization-induced chronic hepatic toxicity, occurring at a median of 2.3 y (range, 6 mo to 5 y) after radioembolization (*15*). In the future, more studies with a longer follow-up duration may be warranted.

One limitation of our study was its retrospective nature. Other limitations were the heterogeneity of the population and follow-up imaging, lack of safety data due to the low number of events, and insufficient statistical power due to the low sample size. Furthermore, the follow-up of 12 mo may be insufficient to fully capture late-onset hepatotoxicity, previously described in the literature (*15*). As most patients were treated within the first week after calibration, our results may not be applicable to treatments performed in the second week after calibration. Also, not all patients were enrolled in the evaluation of tumor response because some patients did not have tumors 2 cm or larger. Finally, ^{99m}Tc-MAA SPECT/CT was used for dosimetry; although this currently is the most accurate approach

for pretherapeutic dose assessment, it may not always accurately reflect intratherapeutic dose distribution.

CONCLUSION

The results of our study indicate a higher response rate and longer global PFS in NEN patients in whom higher tumor doses could be achieved, implying that a higher tumor-absorbed dose may be critical to achieve a treatment response.

DISCLOSURE

Masao Watanabe has a postdoctoral fellowship from Humboldt Foundation. Benedikt Schaarschmidt received a research grant from PharmaCept for an ongoing investigator-initiated study not related to this paper. Wolfgang Fendler reports fees from SOFIE Biosciences (research funding), Janssen (consultant, speaker), Calyx (consultant, image review), Bayer (consultant, speaker, research funding), Novartis (speaker, consultant), Telix (speaker), GE Healthcare (speaker), Eczacıbaşı Monrol (speaker), and Abx (speaker), outside the submitted work. Ken Herrmann reports personal fees from Bayer, SIRTEX, Adacap, Curium, Endocyte, IPSEN, Siemens Healthineers, GE Healthcare, Amgen, Novartis, ymabs, Aktis Oncology, Theragnostics, and Pharma 15; personal fees and other fees from Sofie Biosciences; nonfinancial support from ABX; and grants and personal fees from BTG, outside the submitted work. Manuel Weber reports personal fees from Boston Scientific, Terumo, Advanced Accelerator Applications, IPSEN, and Eli Lilly, outside the submitted work. No other potential conflict of interest relevant to this article was reported.

KEY POINTS

QUESTION: Are tumor doses derived from multicompartment dosimetry predictive of treatment response, PFS, OS, and liver failure in patients with NEN undergoing radioembolization?

PERTINENT FINDINGS: Higher absorbed tumor doses are associated with treatment response and global PFS but not with hepatic PFS and OS. Higher mean doses to the nontumor liver tissue may carry an increased risk of liver decompensation.

IMPLICATIONS FOR PATIENT CARE: Dosimetric parameters derived from multicompartment dosimetry may be helpful to maximize treatment efficacy and safety in NEN patients undergoing radioembolization.

REFERENCES

1. Pavel M, Öberg K, Falconi M, et al. Gastroenteropancreatic neuroendocrine neoplasms: ESMO clinical practice guidelines for diagnosis, treatment and follow-up. *Ann Oncol.* 2020;31:844–860.
2. Lewandowski RJ, Toskich BB, Brown DB, El-Haddad G, Padia SA. Role of radioembolization in metastatic neuroendocrine tumors. *Cardiovasc Intervent Radiol.* 2022;45:1590–1598.
3. Schaarschmidt BM, Wildgruber M, Kloeckner R, et al. ^{90}Y radioembolization in the treatment of neuroendocrine neoplasms: results of an international multicenter retrospective study. *J Nucl Med.* 2022;63:679–685.
4. Salem R, Padia SA, Lam M, et al. Clinical, dosimetric, and reporting considerations for Y-90 glass microspheres in hepatocellular carcinoma: updated 2022 recommendations from an international multidisciplinary working group. *Eur J Nucl Med Mol Imaging.* 2023;50:328–343.
5. Weber M, Lam M, Chiesa C, et al. EANM procedure guideline for the treatment of liver cancer and liver metastases with intra-arterial radioactive compounds. *Eur J Nucl Med Mol Imaging.* 2022;49:1682–1699.
6. Ramdhani K, Bratt AJAT. The evolving role of radioembolization in the treatment of neuroendocrine liver metastases. *Cancers (Basel).* 2022;14:3415.
7. Garin E, Tselikas L, Guiu B, et al. Personalized versus standard dosimetry approach of selective internal radiation therapy in patients with locally advanced hepatocellular carcinoma (DOSISPHERE-01): a randomised, multicentre, open-label phase 2 trial. *Lancet Gastroenterol Hepatol.* 2021;6:17–29.
8. Chansanti O, Jahangiri Y, Matsui Y, et al. Tumor dose response in yttrium-90 resin microsphere embolization for neuroendocrine liver metastases: a tumor-specific analysis with dose estimation using SPECT-CT. *J Vasc Interv Radiol.* 2017;28:1528–1535.
9. Ebbers SC, Roekel CV, Braat MNGJA, Barentsz MW, Lam MGEH, Braat AJAT. Dose-response relationships after yttrium-90-radioembolization with glass microspheres in patients with neuroendocrine tumor liver metastases. *Eur J Nucl Med Mol Imaging.* 2022;49:1700–1710.
10. Watanabe M, Grafe H, Theysohn J, et al. Voxel-based dosimetry predicts hepatotoxicity in hepatocellular carcinoma patients undergoing radioembolization with ^{90}Y glass microspheres. *J Nucl Med.* 2023;64:1102–1108.
11. Lam M, Garin E, Palard-Novello X, et al. Direct comparison and reproducibility of two segmentation methods for multicompartment dosimetry: round robin study on radioembolization treatment planning in hepatocellular carcinoma. *Eur J Nucl Med Mol Imaging.* 2023;51:245–257.
12. Choi H, Charnsangavej C, Faria SC, et al. Correlation of computed tomography and positron emission tomography in patients with metastatic gastrointestinal stromal tumor treated at a single institution with imatinib mesylate: proposal of new computed tomography response criteria. *J Clin Oncol.* 2007;25:1753–1759.
13. Solis-Hernandez MP, Valle AFD, Carmona-Bayonas A, et al. Evaluating radiological response in pancreatic neuroendocrine tumours treated with sunitinib: comparison of Choi versus RECIST criteria (CRIPNET_GETNE1504 study). *Br J Cancer.* 2019;121:537–544.
14. Garin E, Rolland Y, Laffont S, Edeline J. Clinical impact of ^{99m}Tc-MAA SPECT/CT-based dosimetry in the radioembolization of liver malignancies with ^{90}Y-loaded microspheres. *Eur J Nucl Med Mol Imaging.* 2016;43:559–575.
15. Currie BM, Nadolski G, Mondschein J, et al. Chronic hepatotoxicity in patients-with metastatic neuroendocrine tumor: transarterial chemoembolization versus transarterial radioembolization. *J Vasc Interv Radiol.* 2020;31:1627–1635.